Longer Duration of the Weak Stratospheric Vortex During Extreme El Niño Events Linked to Spring Eurasian Coldness

Article *in* Journal of Geophysical Research Atmospheres · July 2020

DOI: 10.1029/2019JD032331

Xin Zhou
Chinese Academy of Sciences

Quanliang Chen
Chengdu University of Information Technology

Mian Xu
Lanzhou University

Sen Zhao
University of Hawaiʻi at Mānoa

JGR Atmospheres

RESEARCH ARTICLE
10.1029/2019JD032331

Special Section:
Long-term Changes and Trends in the Middle and Upper Atmosphere

Key Points:
- We found greater persistence of extreme El Niño signals through the stratospheric pathway to midlatitude Eurasia
- The contribution of the stratospheric pathway is isolated with model and is found to be critical in maintaining the signals
- The prolonged stratospheric pathway of extreme El Niño events can increase the risk of cold spells especially over Eurasia

Supporting Information:
- Supporting Information S1

Correspondence to:
Q. Chen,
chenql@cuit.edu.cn

Citation:
Zhou, X., Chen, Q., Wang, Z., Xu, M., Zhao, S., Cheng, Z., & Feng, F. (2020). Longer duration of the weak stratospheric vortex during extreme El Niño events linked to spring Eurasian coldness. *Journal of Geophysical Research: Atmospheres*, *125*, e2019JD032331. https://doi.org/10.1029/2019JD032331

Received 6 JAN 2020
Accepted 26 JUN 2020
Accepted article online 2 JUL 2020

Author Contributions:
Conceptualization: Xin Zhou
Data curation: Xin Zhou
Formal analysis: Xin Zhou
Investigation: Xin Zhou
Methodology: Xin Zhou
Resources: Xin Zhou
Software: Xin Zhou
Validation: Xin Zhou
Visualization: Xin Zhou
Writing - original draft: Xin Zhou
Writing – review & editing: Xin Zhou

Longer Duration of the Weak Stratospheric Vortex During Extreme El Niño Events Linked to Spring Eurasian Coldness

Xin Zhou[1], Quanliang Chen[1], Zhenglin Wang[1], Mian Xu[2], Sen Zhao[3,4], Zhigang Cheng[1], and Fan Feng[1]

[1]Plateau Atmosphere and Environment Key Laboratory of Sichuan Province, College of Atmospheric Science, Chengdu University of Information Technology, Chengdu, China, [2]Key Laboratory for Semi-Arid Climate Change of the Ministry of Education, College of Atmospheric Sciences, Lanzhou University, Lanzhou, China, [3]CIC-FEMD/ILCEC, Key Laboratory of Meteorological Disaster of Ministry of Education, Nanjing University of Information Science and Technology, Nanjing, China, [4]Department of Atmospheric Sciences, University of Hawai'i at Mānoa, Honolulu, HI, USA

Abstract The stratosphere is a key link between El Niño and Eurasian surface climate in winter. Instead of the amplitude of the stratospheric response discussed by many previous studies, we focus on the persistence of wintertime extreme El Niño impacts through the stratospheric pathway to midlatitude Eurasia in spring. A novel approach is used by running WACCM4 with El Niño forcing imposed only during winter to isolate the stratospheric role in the following spring. We show that a descending signal with a strong deceleration of zonal wind throughout the atmosphere could reach the surface and persist in spring during extreme El Niño events, whereas during moderate El Niño events the signal is generally confined to the stratosphere. Two different mechanisms are involved in maintaining the tropospheric signal of extreme El Niño. Under the westerly regime, the planetary Rossby waves from the wave centers over East Asia and the North Pacific transmit the signals from the stratosphere to the troposphere; and under the easterly regime, strong tropospheric eddy feedback over the midlatitude Atlantic favors the persistence of tropospheric responses during extreme El Niño events. The prolonged stratospheric pathway of extreme El Niño events amplifies and extends the equatorward shift of the midlatitude jet, allowing southward intrusions of cold polar air into Eurasia. Such circulation changes induced by a prolonged stratospheric pathway can cause springtime coldness and daily cold extremes in midlatitude Eurasia.

1. Introduction

The importance of the stratospheric pathway linking El Niño–Southern Oscillation (ENSO) to surface conditions over Eurasia has been highlighted in many studies (e.g., Bell et al., 2009; Butler et al., 2014; Cagnazzo & Manzini, 2009; Fletcher & Cassou, 2015; Ineson & Scaife, 2009; Ortiz Bevia et al., 2010; Toniazzo & Scaife, 2006; Zhang et al., 2016). ENSO extends its signal from the tropical Pacific to the Northern Hemisphere (NH) extratropics by exciting longwave trains in the form of an anomalous Pacific North American (PNA) pattern (Garcia-Herrera et al., 2006) and shortwave trains along the North African-Asian jet (Shaman & Tziperman, 2005; Zhang et al., 2015), with opposite sign during warm El Niño (EN) and cold La Niña (LN) phases in the PNA sector. Constructive interference between EN teleconnections and climatological Rossby waves (Fletcher & Kushner, 2011, 2013; Smith et al., 2010) intensifies the upward propagation of planetary Rossby waves to the stratosphere in the NH during winter, resulting in a warmer and weaker polar vortex (Camp & Tung, 2007; Free & Seidel, 2009; Garcia-Herrera et al., 2006; Garfinkel, Hurwitz, Oman, et al., 2013, Garfinkel, Hurwitz, Waugh, et al., 2013; Lan et al., 2012; Manzini et al., 2006; Ren et al., 2012; Xie et al., 2012). Subsequently, EN-related stratospheric anomalies propagate downward into the troposphere, projecting onto a negative NAO phase, leading to a colder and drier climate in Eurasia during winter than normal (Brönnimann et al., 2007; Kolstad et al., 2010; Perlwitz & Graf, 1995; Thompson et al., 2002). Thus, understanding the coupling between the stratosphere and troposphere is fundamental to improving seasonal prediction at midlatitudes, including cold spells.

The SST patterns of individual EN events may differ, with two main types of EN being defined: the eastern (EP) EN and the central Pacific (CP) EN (Ashok et al., 2007; Kao & Yu, 2009; Kug et al., 2009; Larkin & Harrison, 2005; Yu & Kao, 2007). This diversity may lead to differences in the stratospheric pathway.

However, previous studies are not entirely consistent, as noted by a recent review on ENSO teleconnections to the stratosphere by Domeisen et al. (2019). For example, Hegyi and Deng (2011) found that CP EN leads to an anomalously strong NH stratospheric vortex and is associated with a positive phase of the NAO pattern at the surface. In contrast, Graf and Zanchettin (2012) showed results associating CP EN with the negative phase of the NAO, with the same sign of EP events. Reasons for this discrepancy is not clear yet, but limited number of events (Garfinkel, Hurwitz, Waugh, et al., 2013), large internal variability (Deser et al., 2017), and model independence may count. The magnitude of the EN is also important as the SST pattern. Three extreme EN events (defined as the Niño3.4 index being >2 K; see section 2) have been observed in the satellite era in winter 1982/1983, 1997/1998, and 2015/2016. But there is disagreement on whether the stratospheric response is proportional to the EN magnitude. Nonlinearity is found in Rao and Ren (2016a, 2016b) that moderate EN events are more efficient in modulating the stratospheric vortex than strong EN events, while modeled results in Richter et al. (2015) and Trascasa-Castro et al. (2019) support linear response. Zhou et al. (2018) (hereinafter Zhou18) suggest that the seasonal evolution of the stratospheric response during winter matters when considering the nonlinearity: The results differ for early winter mean and late winter mean. And there are studies found that the anomalous strength of the stratospheric vortex quickly switches from positive to negative between December and January in cases of extreme EN (Ayarzagüena et al., 2018; Calvo et al., 2010; Hardiman et al., 2019), though the reason for the anomalously strong vortex in extreme EN in early winter is not clear yet. These findings highlight the importance of considering seasonal variations when depicting the stratospheric response to EN.

However, most research of the impact of EN on Eurasia via the stratospheric pathway has focused on the linearities/nonlinearities in the magnitude, while the persistence of the impacts has not received much attention. Manzini et al. (2006) mentioned the possibility of a spring signal of EN in the zonal mean zonal wind down to the surface following the stratospheric pathway. Herceg-Bulić et al. (2017) used numerical simulations to show a delayed EN signal in the European spring climate, though it was mainly attributed to atmosphere-ocean interactions in the North Atlantic. For extreme EN events, it is not clear whether their influence on Eurasia can extend to the following spring via the stratospheric pathway. Zhou18 found that the magnitude of the stratospheric response to extreme EN events is more than 4 times larger than that to moderate EN events in late winter and early spring, as stronger upward propagation of planetary waves leads to a weaker northern polar vortex during extreme EN events than during moderate EN events. Nevertheless, the main question remains: Can the impact of winter extreme EN on surface climate extend longer to the following spring through the stratospheric pathway? In this study, we focus on the persistence of the extreme EN events impacts through the stratospheric pathway to midlatitude Eurasia in spring, which have the potential for forecasting improvements.

As mentioned above, the extreme EN stratospheric response is seasonally dependent, so it is important to focus on a single period when depicting the potential downward coupling from the stratosphere to the troposphere. The period investigated in this study is the springtime (March to May). It is important to note that the stratospheric pathway is not the only path by which EN can influence Eurasia: The superposition and interaction of effects from the tropospheric pathway may add complexity and nonlinearity to the system. So, we first isolate the role of the stratospheric pathway before quantifying its contribution and explaining its dynamics. Several different approaches have been applied in previous studies to isolate the role of the stratospheric pathway. Statistical diagnostics using observations cannot clearly isolate the stratospheric signal due to interactions between the stratospheric and tropospheric pathways (Jiménez-Esteve & Domeisen, 2018). The numerical approach can simply omit the stratospheric signal: Newman and Sardeshmukh (2008) used linear inverse models with stratospheric feedback removed; Simpson et al. (2011) and Wu and Smith (2016) shut down the stratospheric pathway in models by applying a nudging method to the stratosphere. In this study, we address this issue with a novel approach using the Whole Atmosphere Community Climate Model version 4 (WACCM4). The prescribed EN-SST forcing in idealized experiments is limited to winter, so that the tropospheric pathway can be ignored ~2 weeks after the termination of the forcing (Jin & Hoskins, 1995), and the lagged response is purely attributed to the stratospheric pathway, which will be illustrated specifically in section 3. By doing so we are able to isolate the stratospheric pathway of EN to the troposphere. We demonstrate a significant longer duration of the extreme EN impacts by the stratospheric pathway in spring, comparted with that of moderate EN events. And we investigate different characteristics of wave activity favoring the persistence of EN impacts under the westerly/easterly regime.

This paper is organized as follows: Model simulations, observational data sets, and reanalysis methods are introduced in section 2. Section 3 confirms that the role of the stratospheric pathway is well isolated. Section 4 presents the springtime signal of extreme and moderate EN signals through the stratospheric pathway based on observations and simulations and discusses associated dynamical mechanisms. Section 5 shows the induced spring coldness over Eurasia. The paper concludes with a summary and discussion in section 6.

2. Model Experiments, Data, and Methodology

2.1. Definition of Extreme and Moderate EN

We adopt the same definition of extreme and moderate events as in Zhou18. Three of the EP events defined by the Cold Tongue and Warm Pool indices (Ren & Jin, 2013) fall into the "extreme" category in our study: the 1982/1983, 1997/1998, and 2015/2016 events, with the Niño3.4 anomaly reaching 2 K (L'Heureux et al., 2017). Three other EP EN events (1986/1987, 1987/1988, and 2006/2007) are identified as "moderate." Composite winter SST anomaly patterns for extreme and moderate ENSO have been shown in our previous work (Figure 1 in Zhou18). Both extreme and moderate EN events exhibit similar EP SST patterns, but the strength of extreme EN events (peak of the Niño3.4 index) is about twice that of the moderate EN events. The composite results are based on a very limited number of events which is insufficient for robust polar stratospheric responses, so the model simulations are involved to overcome the limited availability of observations and isolated the contribution of the stratospheric pathway.

2.2. Model and Experimental Design

The WACCM is a state-of-the-art chemistry-climate model developed at the National Center for Atmospheric Research (NCAR) and can be used as the atmospheric component of the Community Earth System Model (CESM) (Hurrell et al., 2013). WACCM4, the version used in our experiments, has a horizontal resolution of $1.9° \times 2.5°$ and does not include interactive chemistry (Garcia et al., 2007). The vertical resolution is 1.1–1.4 km in the tropical tropopause layer and the lower stratosphere (height below 30 km), with 66 vertical levels extending from the ground to 4.5×10^{-6} hPa (~145 km geometric altitude). For detailed descriptions of the model, see Garcia et al. (2007) and Marsh et al. (2013).

Three experiments with daily output are designed to isolate the role of the stratospheric pathway and analyze the day-to-day propagation of the extreme EN signal and that of the moderate EN. The first is a climatological run using prescribed fixed SSTs of the 12-month seasonal cycle based on the period 1980–2015. The other two have EN-SST forced SSTs in the tropical Pacific (30°S to 30°N, 120–280°E), one using composited extreme EN and one using moderate EN SSTs, and climatological SSTs elsewhere. In the two sensitivity runs, the forcing is limited to December, January, and February of every year and during the rest of the year climatological SSTs are prescribed globally. Hence, the tropospheric pathway is active solely during the DJF season and the following ~2 weeks. After then, only the lagged EN influences through the stratospheric pathway are possible. See Zhou18 for a more detailed description the experimental design. WACCM4 accurately captures the variability and dynamical features of the stratosphere (de la Torre et al., 2012). The seasonal evolution of the circulation anomalies follows the same pattern with decaying amplitudes during springtime (March to May), so a seasonal mean is taken for the period 15 March to 15 May to isolate a critical, consistent dynamical mechanism and to obtain statistical significance in the following analysis, unless specified otherwise.

2.3. Observational Data

SST data were taken from the Hadley Centre Sea Ice and Sea Surface Temperature (HadISST) data set (Rayner et al., 2003), with a horizontal resolution of $1° \times 1°$. The Niño3.4 index is defined by the SST anomalies averaged in the region 5°N to 5°S, from 170°W to 120°W. It is available from the Climate Prediction Center (http://www.cpc.noaa.gov/data/indices/). Daily mean wind, temperature, and geopotential height data were taken from the monthly mean European Centre for Medium Range Weather Forecasting (ECMWF) reanalysis data set (ERA-Interim) for the period 1979–2016 (Simmons, Uppala, & Dee, 2007, Simmons, Uppala, Dee, & Kobayashi, 2007; Uppala et al., 2008) and is obtained from http://apps.ecmwf.int/datasets/. To verify the results obtained using ERA-Interim, data from the NCEPDOE reanalysis were also used. The main results from these two reanalysis data sets are in close agreement, so only the results from the ERA-Interim reanalysis are presented.

2.4. Analysis Methods

Monthly anomalies are calculated by subtracting the long-term mean of each calendar month from each individual month. The linear trends are removed before analysis from the temperature, zonal wind, sea level pressure (SLP), and geopotential height data using linear regression analysis. To avoid possible interference from the Quasi-biennial Oscillation (QBO), biennial circulation anomalies (24–32 months) are filtered out of the temperature and circulation fields. Composite analysis is applied to the stratospheric response during extreme EN and moderate EN events.

Indexes for cold extremes of temperature are used in this study: the percentile index, T10, and the absolute index, TN (Alexander et al., 2006; Zhang et al., 2005). T10 is calculated from the 10th percentile of daily temperature variability for the climatological run, a percentage count of the number of days below the 10th percentile. TN is the seasonal coldest instance of daily temperature and gives absolute extremes in contrast to T10. The absolute index TN reveals intensity, and the percentile index T10 gives a sense of the number of days that are affected by the circulation regimes (Alexander et al., 2006; Frich et al., 2002). As T10 uses a percentile threshold, the actual temperature threshold varies with the seasonal cycle so T10 counts unusually cold days relative to the seasonal cycle.

We apply a series of dynamical diagnostics. The wave activity flux proposed by Takaya and Nakamura (2001) is used to show the propagation features of quasi-stationary Rossby waves in the extratropics. The formulation of the three-dimensional wave activity flux can be expressed as follows:

$$\mathbf{W} = \frac{p\cos\varphi}{2|\mathbf{U}|}\begin{bmatrix} \dfrac{U}{a^2\cos^2\phi}\left[\left(\dfrac{\partial\psi'}{\partial\lambda}\right)^2 - \psi'\dfrac{\partial^2\psi'}{\partial\lambda^2}\right] + \dfrac{V}{a^2\cos\phi}\left[\dfrac{\partial\psi'}{\partial\lambda}\dfrac{\partial\psi'}{\partial\phi} - \psi'\dfrac{\partial^2\psi'}{\partial\lambda\partial\phi}\right] \\ \dfrac{U}{a^2\cos\phi}\left[\dfrac{\partial\psi'}{\partial\lambda}\dfrac{\partial\psi'}{\partial\phi} - \psi'\dfrac{\partial^2\psi'}{\partial\lambda\partial\phi}\right] + \dfrac{V}{a^2}\left[\left(\dfrac{\partial\psi'}{\partial\phi}\right)^2 - \psi'\dfrac{\partial^2\psi'}{\partial\phi^2}\right] \\ \dfrac{f_0^2}{N^2}\left\{\dfrac{\mathrm{U}}{a\cos\phi}\left[\dfrac{\partial\psi'}{\partial\lambda}\dfrac{\partial\psi'}{\partial z} - \psi'\dfrac{\partial^2\psi'}{\partial\lambda\partial z}\right] + \dfrac{V}{a}\left[\dfrac{\partial\psi'}{\partial\phi}\dfrac{\partial\psi'}{\partial z} - \psi'\dfrac{\partial^2\psi'}{\partial\phi\partial z}\right]\right\} \end{bmatrix} + \mathbf{C}_U M, \tag{1}$$

where $\mathbf{U}$ is the background flow ($\mathbf{U} = U_{\boldsymbol{i}} + V_{\boldsymbol{j}}$), $\mathbf{C}_U$ is the phase speed relative to the background flow $\left(\mathbf{C}_U = \mathbf{C}_p\dfrac{U}{|U|}\right)$. $\mathbf{W}$ is the wave activity flux parallel to the group speed, M is the wave activity pseudomomentum, and ψ' is the quasi-geostrophic perturbation stream function. The primes represent perturbations from the climatological means.

The interactive processes between the transient eddies on the background quasi-stationary mean flow is diagnosed by the extended Eliassen-Palm (EP) flux (Hoskins et al., 1983; Plumb, 1985; Trenberth, 1986). The horizontal flux components of the extended EP flux from Trenberth (1986) is adopted:

$$E_u = \left[\frac{1}{2}\times\left(\overline{v'^2} - \overline{u'^2}\right)\vec{\mathrm{i}}, -\overline{u'v'}\,\vec{\mathrm{j}}\right]\times\cos\varphi, \tag{2}$$

where u' and v' represent synoptic-scale zonal and meridional winds, respectively, the overbars denote time average, and φ is latitude. To obtain the synoptic-scale disturbances, a Butterworth band-pass filter is applied to retain fluctuations with 2–8 day period (Murakami, 1979).

The maximum Eady growth rate (EGR) is calculated to study changes in baroclinicity and to analyze the feedback on the circulation changes. It is given by Vallis (2013):

$$\sigma_E = 0.3098\,\frac{|f|\left|\dfrac{\partial u}{\partial z}\right|}{N}, \tag{3}$$

where N is the buoyancy frequency, g is the acceleration due to gravity, and f is the Coriolis parameter.

3. Isolating the Role of the Stratospheric Pathway

As mentioned above, it is important to isolate the role of the stratospheric pathway before quantifying its contribution and attempting to understand its dynamics. The experiments using WACCM4 allow us to

10.1029/2019JD032331

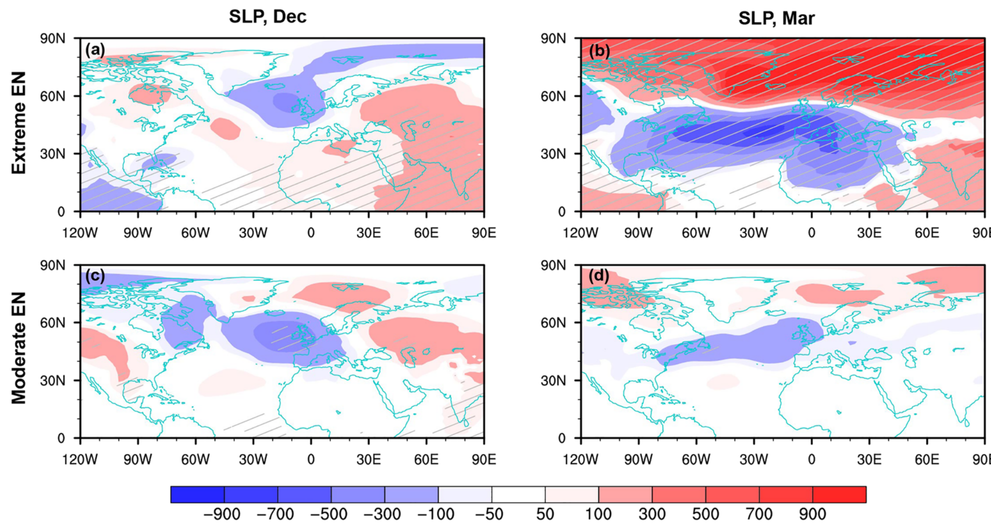

Figure 1. Modeled (left) December and (right) March sea level pressure (SLP) in the North Atlantic for (a, b) extreme EN and (c, d) moderate EN, using 30 winters simulated by WACCM4. SLP anomalies that are significant at the 95% confidence level (Student's *t* test) are indicated by hatching.

achieve this goal. We first need to carefully check that whether the role of the stratospheric pathway is well isolated. Following Hardiman et al. (2019), we compared the SLP response in the North Atlantic for December, the first month when the EN-SST forcing is imposed, and March, a month after the termination of the EN-SST forcing (Figure 1). As expected, the tropospheric pathway dominates in early winter leading to the transatlantic wavelike response to extreme EN. In springtime, however, the SLP response shows an anomalously negative NAO, indicating the stratospheric pathway dominates. In the moderate EN case, the SLP response is in good agreement with previous studies, with an anomalously negative NAO in early winter, which becomes weak and insignificant in spring. The simulated wavelike pattern in December for extreme EN events is not as significant as in Figure 4 of Hardiman et al. (2019). This is because our simulations are atmosphere-only experiments, rather than coupled ones as in Hardiman et al. (2019). The atmosphere-only configuration cannot fully represent the tropospheric pathway because the EN-induced SST variations in oceans other than the eastern Pacific are not captured.

We have demonstrated that in spring the stratospheric pathway dominates the EN signals. Next, the possible existence of a tropospheric pathway in the model results during spring is carefully evaluated to ensure that the effects in spring are attributable solely to the stratospheric pathway. Previously proposed mechanisms of the tropospheric pathway include a modulation by the delayed North Atlantic SST warming prolonging the impacts to late spring (Toniazzo & Scaife, 2006), influences from a climatological shift in the NAO phase

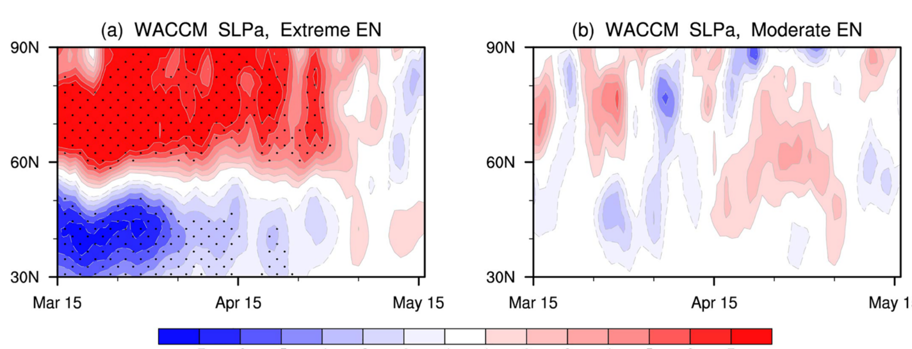

Figure 2. Subseasonal evolution of zonal averaged SLP anomalies (units: hPa) over the North Atlantic (80°W to 30°E) region for (a) extreme EN and (b) moderate EN springs. SLP anomalies that are significant at the 95% confidence level (Student's *t* test) are stippled.

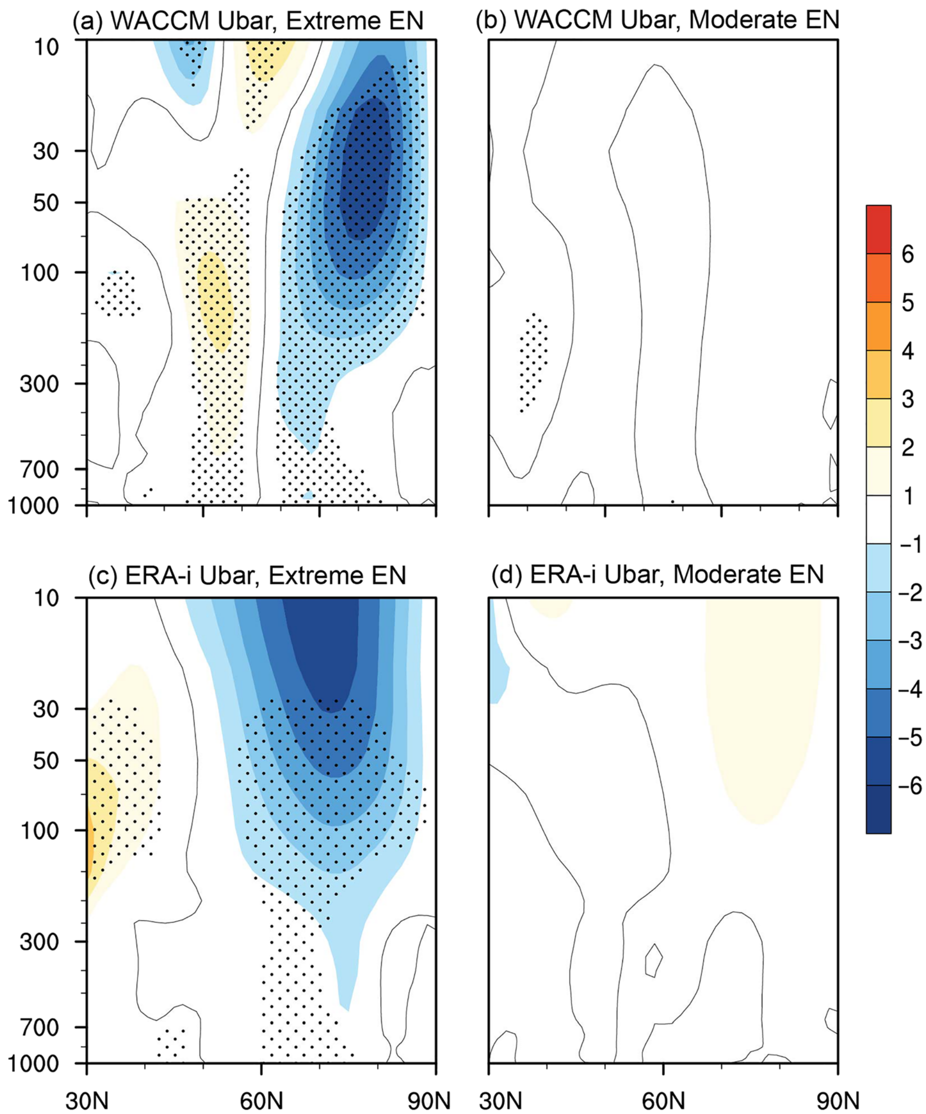

Figure 3. Anomalous zonal wind (contours, negative dashed; units: m s^{-1}) composites of (left) extreme EN and (right) moderate EN events in spring based on (a, b) WACCM4 simulations, and (c, d) ERA-Interim data for 1979–2016. Wind anomalies that are significant at the 95% confidence level (Student's *t* test) are stippled. Before performing the composite analysis, QBO is removed from the ERA-Interim data.

(Geng et al., 2017), and a downstream extension of the PNA wave train carrying energy and momentum along the subtropical jet reaching the North Atlantic and Eurasia in winter (Cassou & Terray, 2001; Jiménez-Esteve & Domeisen, 2018; Li & Lau, 2012; Merkel & Latif, 2002; Pohlmann & Latif, 2005). These are next considered individually. First, the existence of a delayed tropical North Atlantic SST warming can be excluded, because the sensitivity runs are prescribed with climatological SST except in the tropical Pacific. As to the second mechanism proposed by Geng et al. (2017), the temporal evolution of zonal mean SLP anomalies over the North Atlantic region (80°W to 30°E) in spring based on WACCM4 simulations are shown in Figure 2. There is no subseasonal NAO phase reversal in this period (15 March to 15 May) for both extreme EN and moderate EN: Significant positive SLP anomalies north of 50°N and negative SLP anomalies to the south are evident throughout the season for extreme EN, while the anomalies for moderate EN are not significant. Third, the downward extension of the PNA pattern can also be excluded, because there is no anomalous eastward propagation of wave activity from the Pacific to the Atlantic in spring. This result will be specifically analyzed in section 4 when discussing the dynamical mechanisms.

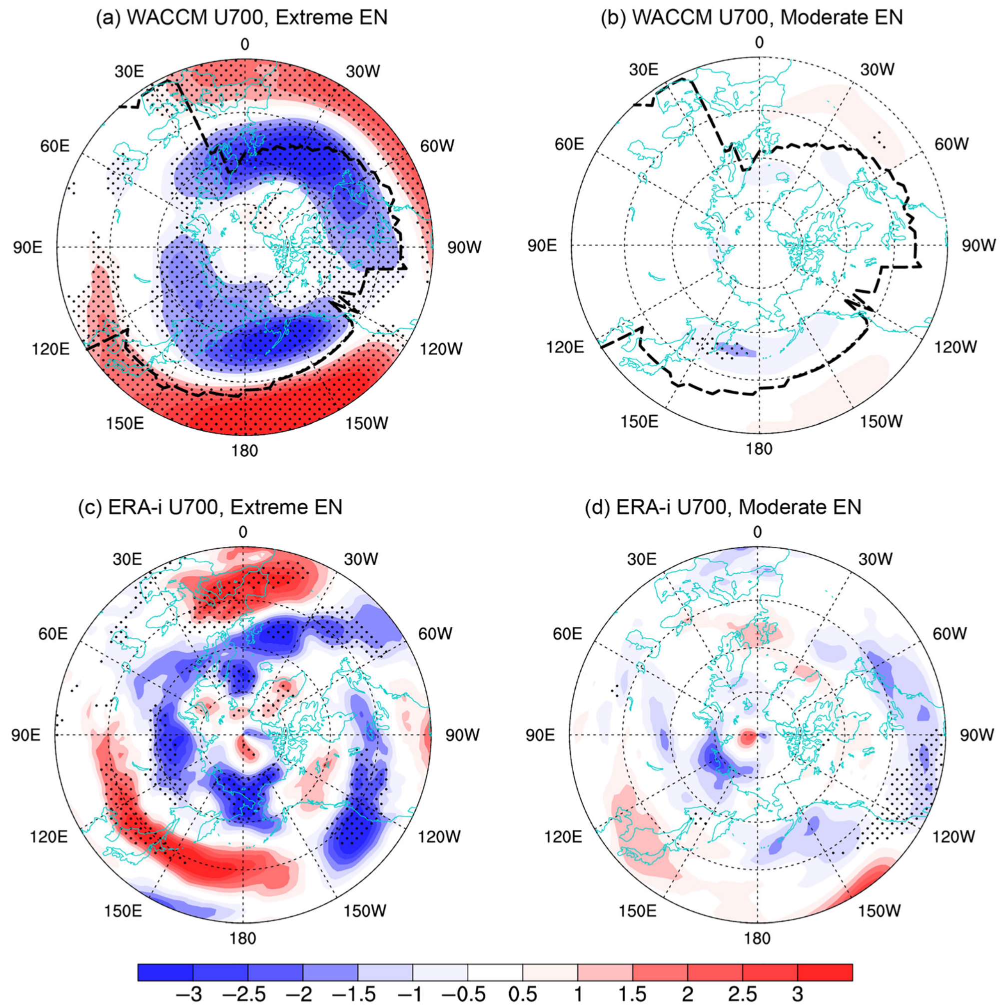

Figure 4. The 700-hPa anomalous zonal wind composites (units: m s^{-1}) for (a) extreme EN and (b) moderate EN in spring based on (top) WACCM4 simulations and (bottom) ERA-Interim from 1979–2016. The dashed lines in (a) and (b) are the position of westerly jet axis in the control run. Wind anomalies that are significant at the 95% confidence level (Student's *t* test) are stippled.

Thus, we have determined that the signal in spring can be attributed solely to the stratospheric pathway. The influence of the stratospheric pathway is underestimated here, because we only consider the lagged response of winter EN-SST forcing. However, this is an effective way to do a minimal estimation of the contribution from the stratospheric pathway.

4. More Persistent Stratospheric Pathway of Extreme EN Events in Spring

A warmer and weaker stratospheric vortex has been observed in late winter and early spring for extreme EN events (Figures 9 and 10 in Zhou18). The persistence of the signal in the troposphere in spring is diagnosed by latitude-pressure sections of the zonal mean zonal wind and maps of the low-level tropospheric zonal wind. Modeled patterns from WACCM4 averaged from 15 March to 15 May (Figures 3a and 3b) show that during extreme EN events, significant negative wind anomalies descend to the surface in spring throughout the atmosphere at high latitudes (60–90°N). The weakening of midlatitude westerlies in the troposphere maintains a significant signal during spring. However, in the moderate EN case the signal is not evident in the zonal mean results. Composite results based on ERA-Interim from 1979 to 2016 (Figures 3c and 3d) are in good agreement with the simulations. Significant negative zonal wind anomalies are observed in the lower troposphere in the extreme EN case but disappear in the moderate EN case. Only in the case of extreme EN events can a significant and strong signal persist in spring in the troposphere.

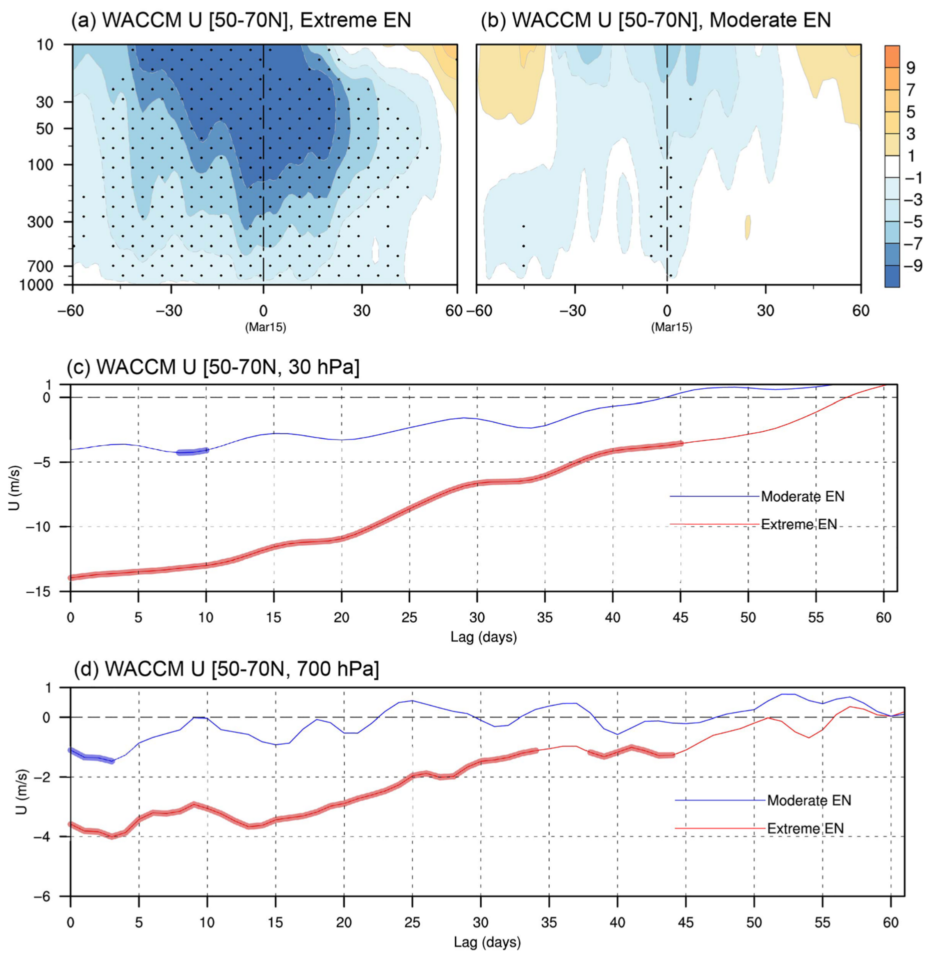

Figure 5. Evolution of zonal mean zonal wind anomaly (units: m s^{-1}) averaged between 50° and 70°N for (a) extreme EN and (b) moderate EN, based on WACCM4 simulations; time series of zonal mean zonal wind anomaly (units: m s^{-1}) averaged between 50°N and 70°N at (c) 30 hPa and (d) 700 hPa. Wind anomalies that are significant at the 95% confidence level (Student's *t* test) are stippled in (a) and (b). The blue line in (c) and (d) indicates moderate EN event behavior and red line indicates extreme EN events. Thicker lines indicate statistically significant anomalies with a confidence of 95%.

The modeled descending signals in the 700-hPa zonal wind for extreme and moderate EN are shown in Figures 4a and 4b. There are strong decreases (increases) in zonal wind over 50–70°N (0–30°N) in the Pacific and Atlantic during extreme EN springs, indicating an equatorward shift of the midlatitude jet. More specifically, the prevailing westerly wind in the upper troposphere blowing across the subpolar region from the North Atlantic to Europe and the Far East, which is closely linked to the surface climate over Eurasia, is dramatically weakened by ~5 m s^{-1} during extreme EN events. The jet response is much weaker and only visible in the Pacific during moderate EN events. Analogous composited maps of midlatitude tropospheric jet anomalies based on ERA-Interim (1979–2016) are shown in Figures 4c and 4d. Consistent with the modeled patterns, there is a significant deceleration of the midlatitude jet, especially in the North Pacific and North Atlantic. However, the eastward extension of the negative jet anomalies reaching the west coast of the Atlantic indicates a contribution from the tropospheric pathway in the composited results using ERA-Interim. Hence, although the composites based on reanalysis data are used to confirm the modeled patterns, the following analysis of the duration of extreme EN signal via the stratospheric pathway and the associated dynamical mechanisms are based on modeled results only.

Figure 5 shows the evolution of the midlatitude jet deceleration for extreme and moderate EN. The day 15 March is marked as the beginning date (day 0) of the persistence calculation. It is chosen in order to identify the contribution of the stratospheric pathway solely as mentioned above. At this point, the downward

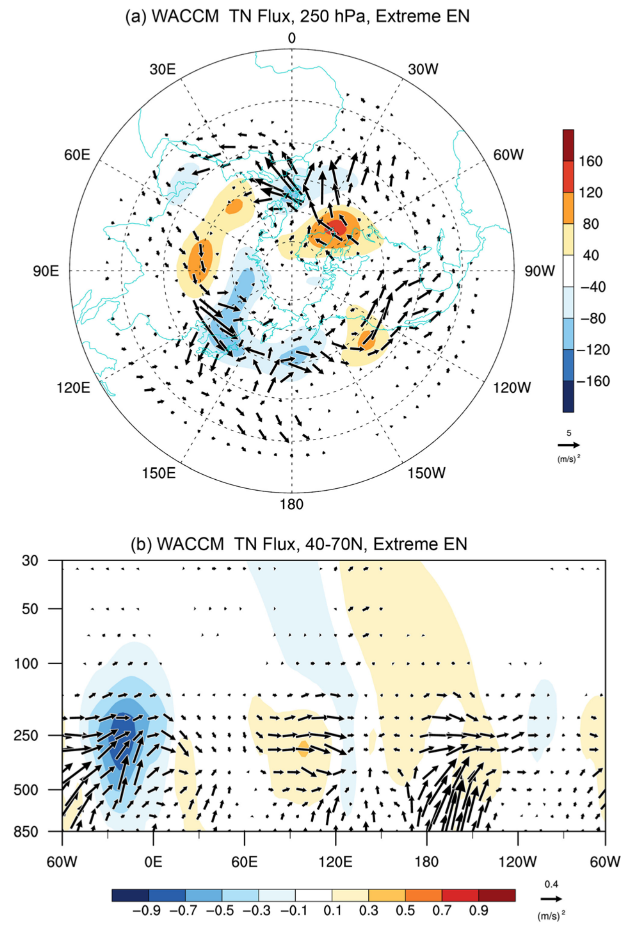

Figure 6. A 250-hPa horizontal wave activity flux (F_x, F_y) (vectors; units: $m^2\ s^{-2}$) and the eddy geopotential height (color shading; units: m) for extreme EN under the westerly regime. (b) Height-longitude cross section of the wave flux averaged over 40–70°N, and vectors show the (F_x, F_z) and color shading indicates the meridional component F_y of the TN flux. The wave flux is multiplied by the square root of 1,000/pressure (hPa) to better demonstrate the waves in the stratosphere. Figures for the moderate case with no obvious response are omitted.

propagating signal via the stratospheric pathway develops to its maximum for both extreme and moderate EN. In case of extreme EN, the amplitude of jet response in the stratosphere maintains a significant value even at Day 45 and gradually decreases to zero till Day 60; the signal near the surface lasts for about one and a half months. However, during moderate EN the signal soon disappears throughout the atmosphere. More clearly, the time evolution of the jet response at middle stratosphere (30 hPa) and lower troposphere (700 hPa) are shown in Figures 5c and 5d. In the middle stratosphere, the jet anomaly for extreme EN is slowly recovering from 15 m s^{-1}, with significant value until day 45; while it is generally insignificant for moderate EN (less than 5 m s^{-1}). At lower-tropospheric level, the significant anomaly lasts ~43 days for extreme EN, in contrast to just 3-day significant value for moderate EN which quickly decreases to zero.

Now we have confirmed a more persistent signal of extreme EN events in model simulations and observations in spring. This raises the question of why extreme EN events are able to maintain strong signals at lower levels for longer duration. Despite the growing body of observational and modeling evidence for a stratospheric influence on tropospheric flow, the mechanism of the stratosphere's downward impact on the troposphere is not yet fully understood. The wave-breaking and reflecting behavior differs under different regimes of stratospheric polar vortex circulation (Graf et al., 2014). That is, planetary-scale waves can only propagate into the westerly winds of the stratospheric polar vortex; while they are trapped in the lower atmosphere when prevailing stratospheric winds are easterly. The metric of 10 hPa 60°N zonal mean zonal wind is used to diagnose the day of the final warming when the polar vortex dissipates and easterlies develop (Butler et al., 2015; Charlton & Polvani, 2007; Lee & Butler, 2020). The last day of zonal mean westerlies is around the end of April (Day 46) for extreme EN (Figure S1 in the supporting information), ~18 days longer than that of climatology (12 April). This implies that a longer persistence for extreme EN impacts may be due to longer basic state favoring the vertically propagating planetary waves, as well as stronger wave source manifested as a deeper Aleutian Low (Figure 5c). Then all days in this period (15 March to 15 May) in each year are assigned to easterly/westerly regime based on the last day of zonal mean westerlies, so that we can clearly separate the processes in the two regimes. We next first consider the contribution of planetary waves in maintaining the signals under the westerly regime, and then illustrate the tropospheric eddy feedback under the easterly regime.

Figure 6a shows the horizontal wave activity flux and wave geopotential height anomalies (Z*; Z* indicates that the zonal mean has been removed) at 250 hPa for extreme EN. Figures for moderate EN case with no noticeable wave activity are omitted here for conciseness. During extreme EN events, the anomalous center of the Aleutian low in winters now shifts to East Asia, indicating a westward tilt of the upward wave propagation center. Importantly, there are strong poleward propagating waves from this wave center, which is responsible for an anomalously weaker tropospheric vortex. Another strong wave center is over the North Atlantic, propagating to the west coast of Europe. Figure 6b shows the longitude-height cross section of the planetary waves averaged over 40–70°N. There is a coherent upward source of wave activity in East Asia and the North Pacific (90–150°E) and a strong equatorward propagation of the planetary wave at the upper-level troposphere over the Atlantic (60–90°W). The upward propagating planetary waves over East Asia and the North Pacific help to sustain an anomalously weaker stratospheric vortex. The planetary waves over the North Atlantic wave center bend south in the troposphere, giving rise to tropospheric geopotential height anomalies over the Atlantic (Figure 6a). Note that no noticeable waves propagate from the Pacific across the Americas to the Atlantic. This further confirms the assertion of section 3 that the impact of the tropospheric pathway in producing the downward extension of the PNA pattern can be excluded.

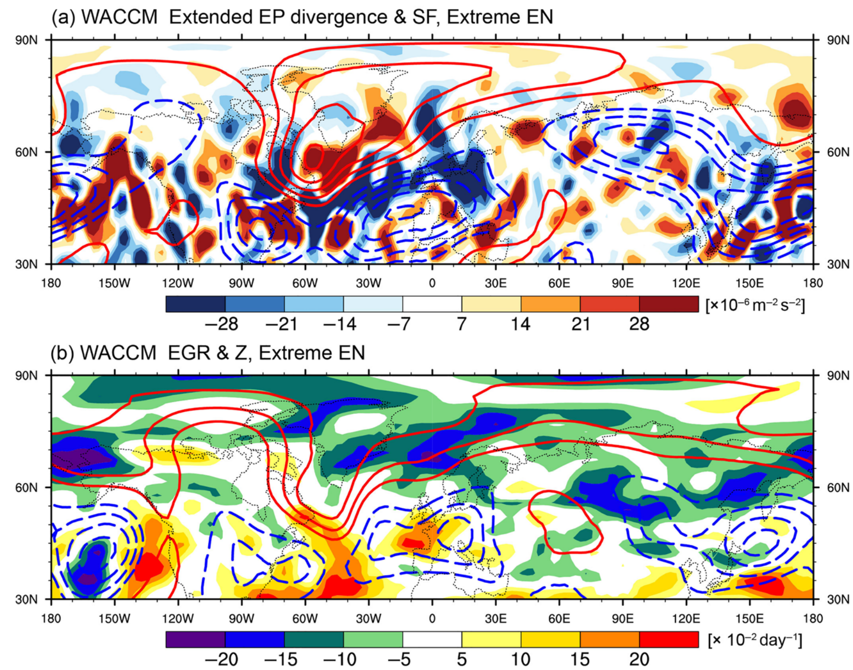

Figure 7. The 250-hPa (a) anomalous extended EP flux divergence (shading; units: 10^{-6} m^2 s^{-2}) and anomalous stream function (contour; interval: 10^6 m^2 s^{-1}), (b) anomalous EGR (shading; units: 10^{-6} m^2 s^{-2}) and anomalous geopotential height (contour; interval: 25 m) under the easterly regime for extreme EN. Figures for the moderate case with no obvious response are omitted.

Under the easterly regime, the anomalous upward propagating wave activity is concentrated mostly in the troposphere and is muted in the stratosphere (not shown). In the troposphere, the signal is maintained locally by positive feedback between the transient eddies and the mean flow (Song & Robinson, 2004). Figure 7a demonstrates the anomalies of 250-hPa stream function and divergence of extended EP flux. The easterly anomaly at the southern flank of the anomalous anticyclone over the North Atlantic suggests equatorward shift of the midlatitude Atlantic jet (Figure 4a), giving rise to the emergence of the local transient eddy flux convergence around 70°W, 50°N (Figure 7a). The convergence of the transient eddy flux lead to an anomalous anticyclone (cyclone) to its north (south) and decelerates the eastward wind, which further attenuates the midlatitude Atlantic jet and in turn increase the flux convergence. This is coherent with previous findings in Zhang et al. (2019) reporting a change in the tropospheric jet over the North Pacific Ocean due to weakening of winter stratospheric vortex. The positive feedback mechanism between transient eddies and the mean flow makes a contribution to a longer duration of the tropospheric circulation anomaly. Figure 7b shows the anomalous geopotential height and anomalous EGR for extreme EN. EGR is related to vertical shear of wind and is a measure of the baroclinic instability. The southward shift of the subtropical jet is corresponding to a general southward shift of the baroclinicity during extreme EN events, manifested as positive anomalies of EGR over the extratropical Atlantic and Pacific region. In addition, the anomaly dipole of EGR pattern is generally matching the geopotential anomaly pattern. The anomalous EGR is larger (smaller) in the lower (upper) troposphere (not shown). This indicates a positive feedback in the troposphere: less synoptic-scale eddies tend to form in the region of negative EGR anomalies at middle-to-high latitudes (60–90°N), thus the vertical wind shear and the baroclinicity weakens, contributing to maintaining an equivalent barotropic structure of the low-frequency atmospheric flow at middle-to-high latitudes by balancing some of the strong damping effect of surface friction (Lorenz & Hartmann, 2001).

In summary, we have discussed two different mechanisms acting constructively, favoring the persistence of EN impacts. When westerlies prevail, the planetary waves propagating northward over the East Asia and the North Pacific wave center and the waves bending south from the North Atlantic wave center are critical in transmitting the stratospheric signal to the troposphere, giving rise to the tropospheric geopotential height anomalies and the weakening of westerlies. After the final breakdown of polar vortex, the positive

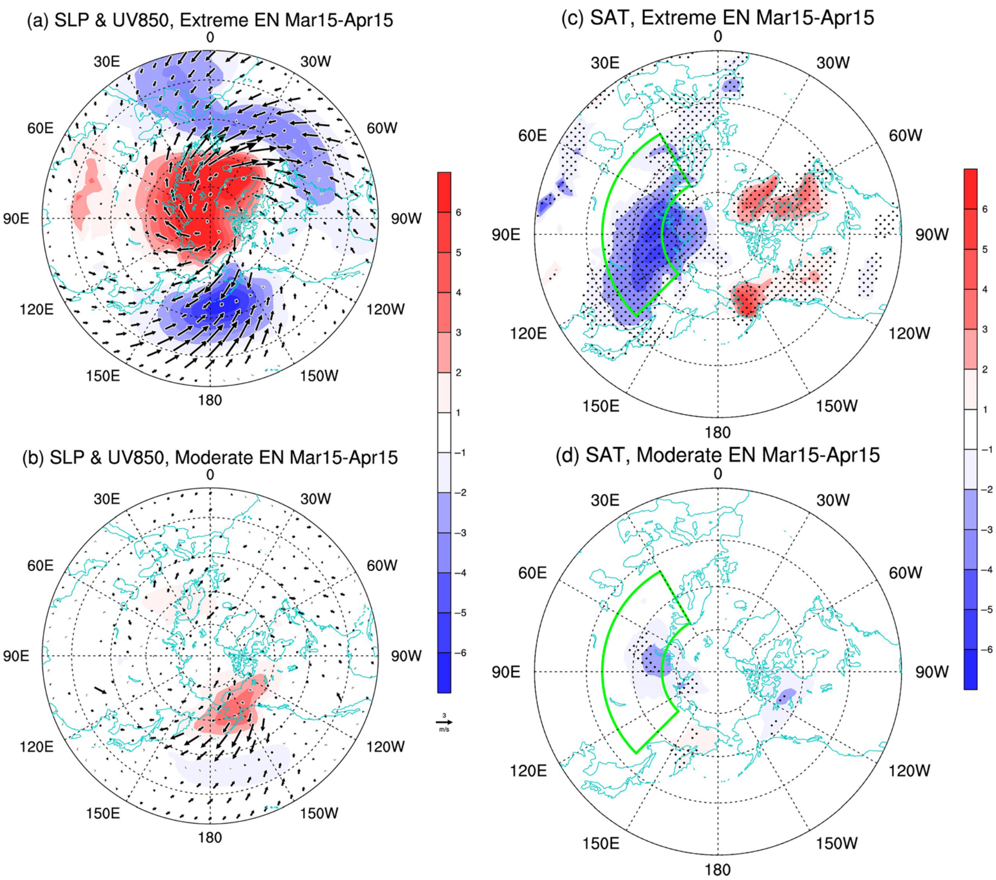

Figure 8. (a) and (b) SLP (shading; units: hPa) and 850-hPa wind (vector; units: m s^{-1}) response to extreme and moderate EN events in spring. (c) and (d) As in (a) and (b) but for SAT response (units: K). SAT anomalies that are significant at the 95% confidence level (Student's *t* test) are stippled. The green box indicates regions over northern Eurasia (50–70°N, 30–130°E).

feedback between transient eddies and the mean flow also favors the persistent weakening of the tropospheric westerlies. These two processes combine constructively to maintain significant values of extreme EN signals for longer duration in the troposphere in spring.

5. Links to Surface Temperature Over Eurasia

The variation in the westerly jet stream can directly affect Eurasian winter surface weather and has been linked with extreme weather and climate events over Eurasia (Kolstad et al., 2010; Tomassini et al., 2012). To address the surface impacts of extreme EN events via the stratospheric pathway, we first show the low-level circulation and temperature response to extreme and moderate EN events, averaged in spring (Figure 8). The following analysis is based on the WACCM4 simulations, because the composites based on reanalysis data sets involve a tropospheric contribution, as discussed above. The small number of events (three extreme EN events and three moderate EN events) compared with the large internal climate variability in Eurasia also makes it difficult to obtain robust results. A dominant role of the North Atlantic pressure seesaw, indicating a negative NAO pattern, is evident during extreme EN springs. The concurrent negative NAO phase and weakened Atlantic westerlies allow southward intrusions of cold polar air into Eurasia and inhibit warm air transport from the Atlantic Ocean toward Europe. This is consistent with the studies cited above suggesting a negative NAO induced by EN via the stratospheric pathway, although previous work has generally focused on EN winter and we focus on the spring following an extreme EN winter. As expected, extreme EN events coincide with anomalously cold surface air temperatures (SAT) in northern Eurasia (green box in Figure 8; 50–70°N, 30–130°E), whereas Canada is anomalously warm. In contrast, during

10.1029/2019JD032331

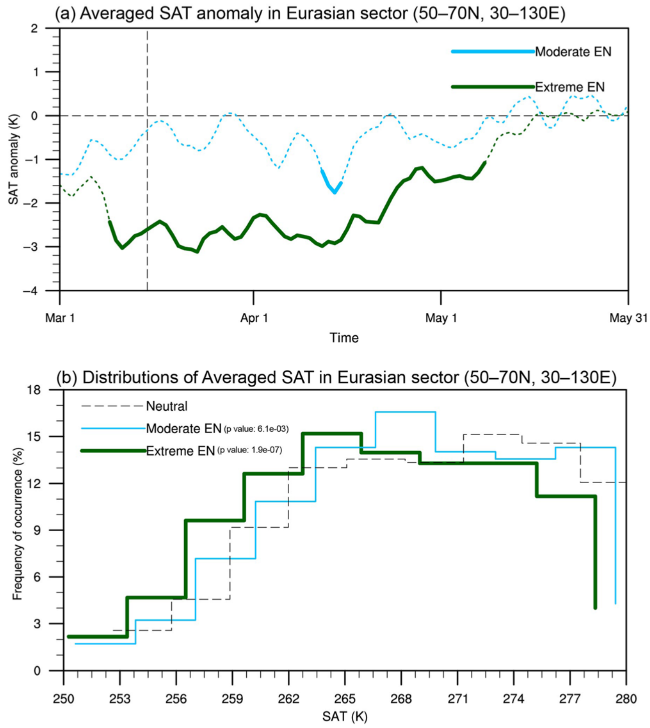

Figure 9. (a) Time series of regional mean SAT anomaly (units: K) in Eurasia (50–70°N, 30–130°E). (b) The distribution of regional mean SAT in Eurasia in spring. The blue and green lines in (a) indicate the response to moderate and extreme EN events, respectively. Solid line segments in (a) highlight regional mean SAT anomalies that are statistically significant at the 95% confidence level. The dashed black, solid blue, and solid green lines in (b) indicate PDFs of SAT for neutral ENSO, extreme EN, and moderate EN events, respectively. The PDFs for extreme EN and moderate EN are statistically different from that for neutral ENSO using a Kolmogorov-Smirnov test ($p < 0.01$).

moderate EN events, the responses of low-level temperature and circulation are rather weak, with a barely evident signal in the North Pacific. The cold response almost completely disappears leaving only a sporadic signal confined to the polar region. These results suggest that a more-persistent stratospheric pathway during extreme EN events acts to enhance and prolong the negative NAO pattern at the surface, resulting in an enhanced surface cooling response over Eurasia in spring.

We further quantify the subseasonal variance of the Eurasian SAT induced by the stratospheric pathway of extreme EN events and inspect its relationship with the spring SAT cold extremes. Figure 9 shows the time evolution of the regional mean SAT anomaly and the probability distribution functions (PDFs) of SAT for extreme and moderate EN events. Consistent with a more persistently weakened Atlantic jet and negative NAO phase, the SAT anomaly over Eurasia maintains a significant low value around −4 K from 15 March to the end of April, and slowly recovers to zero at the end of May. However, during moderate EN events, the regional mean SAT anomaly is generally insignificant. Compared with the neutral ENSO and moderate EN distribution, the PDF for extreme EN events shows a shift of the mean value to the colder side with a slight increase in skewness but no significant difference in variance. This implies that the occurrences of spring cold extremes may increase after extreme EN winters.

We now discuss the extent to which Eurasian cold extremes are affected differently than during the neutral-winter state. As stated above, the T10 index is a count of the percentage of days in which the daily mean temperature is colder than the 10th percentile. TN is the coldest instance of daily mean temperature, which reveals intensity. As can be seen in the top panel of Figure 10, during extreme EN events there is a strong regional increase of cold spring days (T10) in most of Eurasia, accompanied by a tendency of the coldest day (TN) to be even colder. Specifically, there is an increase of up to 12–15% in frequency of cold extremes in Northern Russia and extremely cold days average up to 3 K lower during extreme EN springs. However, during moderate EN events (bottom panel of Figure 10) there is a slight increase in cool days (T10) and a small decrease in the lowest temperature (TN), but these are generally statistically insignificant. Thus, these results

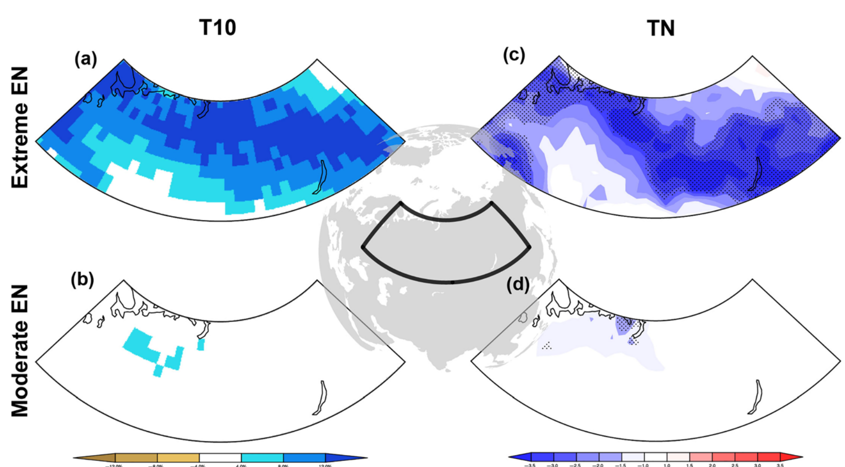

Figure 10. Difference of mean (a, c) extreme EN and (b, d) moderate EN events from the climatological mean (30-year mean of control run) for (a, b) the frequency of the occurrence of cold extremes, and (c, d) the temperature of the coldest day in spring. T10 shows the change in the 10th percentile and TN shows the response of the seasonal coldest night. Temperature anomalies that are significant at the 95% confidence level (Student's t test) are stippled.

indicate that extreme EN events with a persistently weak stratospheric vortex have pronounced impacts on spring coldness in Eurasia.

6. Summary and Discussion

A stratospheric pathway links EN to NH surface climate in winter. Here, we focus on the persistence of extreme EN impacts on Eurasian climate in spring through this stratospheric pathway, with a novel approach using model simulations to isolate the stratospheric role. We find that extreme EN events can induce a more persistent weak stratospheric vortex than moderate EN events, based on observations derived from reanalysis data sets and numerical experiments using WACCM4. A descending signal that reaches the surface to give strong negative zonal wind anomalies throughout the atmosphere maintains longer duration in spring during extreme EN events, while during moderate EN events the signal is insignificant. The explanation for the tropospheric signals of extreme EN involving constructive interference of two different mechanisms are proposed. Under the westerly regime, planetary wave activity centered in the East Asia and North Pacific region, and in the Atlantic region is important in maintaining stratospheric signals and transmitting the signals to the troposphere. Under the easterly regime, strong tropospheric eddy feedback also favors the persistence of the tropospheric response.

The prolonged stratospheric pathway during extreme EN events leads to a persistence to May of negative NAO phase at the surface concurrent with a low-level jet deceleration, allowing southward intrusions of cold polar air into Eurasia, and inhibiting warm air transport from the Atlantic Ocean toward Europe. Hence, a more-persistent weak stratospheric vortex during extreme EN events induces a springtime cold anomaly and daily cold extremes in midlatitude Eurasia.

Geng et al. (2017) have also reported that extreme EN events are associated with cooling in northern Europe and East Asia, but they found no significant stratospheric downward propagation in observations (their Figure S5). The difference may be due to the time period they considered (December to January), as the downward migration may occur in late winter and early spring. Zhou18 compared the magnitude of stratospheric response to extreme EN and moderate EN in winter, but the current study focus on the springtime persistence of extreme EN via the stratospheric pathway and its influences on surface climate over Europe. In other words, Zhou18 discussed the bottom-up process while this study further investigates the top-down effect and in particular its persistence in spring. Recently, Hardiman et al. (2019) found the Atlantic MSLP response to strong LN is a positive NAO which is different from the wavelike response for strong EN in January to February, and they attributed the asymmetry to the predominance of the stratospheric pathway for LN but the tropospheric pathway for EN. We did not include extreme LN events in study and only discussed the role of the stratospheric pathway in favoring a more persistent surface impact in spring for extreme EN. Results presented here suggest that the stratospheric pathway is important in linking extreme EN events with midlatitude circulation and may be of great potential for seasonal prediction for Eurasia.

Data Availability Statements

The reanalysis and observational data sets used here are publicly available and properly cited. The NCEPDOE Reanalysis was obtained from NOAA and is available at this site (http://www.esrl.noaa.gov/psd/data/gridded/). The ERA-Interim reanalysis was obtained from this site (http://apps.ecmwf.int/datasets/). The HadISST from the Met Office Hadley Centre is available at this site (http://www.metoffice.gov.uk/hadobs/hadisst/data/download.html). The numerical simulation data using CESM-WACCM4 from NCAR employed in this research is available online (https://doi.org/10.6084/m9.figshare.11479113).

Acknowledgments
We thank Fei Xie and Jiaqing Xue for constructive comments that helped to improve the manuscript. We would also like to thank William Randel and three anonymous reviewers for their valuable suggestions and comments, which have led to considerable improvements in this work. This work was jointly supported by the National Natural Science Foundation of China (41905037, 41805054, 41875108, and 41971026), and the National Key Research and Development Program on Monitoring, Early Warning and Prevention of Major Natural Disaster (2018YFC1506006).

References

Alexander, L., Zhang, X., Peterson, T., Caesar, J., Gleason, B., Klein Tank, A., et al. (2006). Global observed changes in daily climate extremes of temperature and precipitation. *Journal of Geophysical Research*, *111*, D05109. https://doi.org/10.1029/2005JD006290
Ashok, K., Behera, S. K., Rao, S. A., Weng, H. Y., & Yamagata, T. (2007). El Niño Modoki and its possible teleconnection. *Journal of Geophysical Research*, *112*, C11007. https://doi.org/10.1029/2006JC003798
Ayarzagüena, B., Ineson, S., Dunstone, N., Baldwin, M., & Scaife, A. (2018). Intraseasonal effects of El Niño–Southern Oscillation on North Atlantic climate. *Journal of Climate*, *31*(21), 8861–8873. https://doi.org/10.1175/JCLI-D-18-0097.1
Bell, C. J., Gray, L. J., Charlton-Perez, A. J., Joshi, M. M., & Scaife, A. A. (2009). Stratospheric communication of El Nino teleconnections to European winter. *Journal of Climate*, *22*(15), 4083–4096. https://doi.org/10.1175/2009JCLI2717.1

Brönnimann, S., Xoplaki, E., Casty, C., Pauling, A., & Luterbacher, J. (2007). ENSO influence on Europe during the last centuries. *Climate Dynamics*, *28*(2–3), 181–197.

Butler, A. H., Polvani, L. M., & Deser, C. (2014). Separating the stratospheric and tropospheric pathways of El Nino–Southern Oscillation teleconnections. *Environmental Research Letters*, *9*(2), 024014. https://doi.org/10.1088/1748-9326/9/2/024014

Butler, A. H., Seidel, D. J., Hardiman, S. C., Butchart, N., Birner, N., & Match, A. (2015). Defining sudden stratospheric warmings. *Bulletin of the American Meteorological Society*, *96*(11), 1913–1928. https://doi.org/10.1175/BAMS-D-13-00173.1

Cagnazzo, C., & Manzini, E. (2009). Impact of the stratosphere on the winter tropospheric teleconnections between ENSO and the North Atlantic and European region. *Journal of Climate*, *22*(5), 1223–1238. https://doi.org/10.1175/2008JCLI2549.1

Calvo, N., Garcia, R. R., Randel, W. J., & Marsh, D. R. (2010). Dynamical mechanism for the increase in tropical upwelling in the lowermost tropical stratosphere during warm ENSO events. *Journal of the Atmospheric Sciences*, *67*(7), 2331–2340. https://doi.org/10.1175/2010JAS3433.1

Camp, C. D., & Tung, K. K. (2007). Stratospheric polar warming by ENSO in winter: A statistical study. *Geophysical Research Letters*, *34*, L04809. https://doi.org/10.1029/2006gl028521

Cassou, C., & Terray, L. (2001). Dual influence of Atlantic and Pacific SST anomalies on the North Atlantic/Europe winter climate. *Geophysical Research Letters*, *28*(16), 3195–3198. https://doi.org/10.1029/2000GL012510

Charlton, A. J., & Polvani, L. M. (2007). A new look at stratospheric sudden warmings. Part I: Climatology and modelling benchmarks. *Journal of Climate*, *20*, 449–469.

de la Torre, L., Garcia, R. R., Barriopedro, D., & Chandran, A. (2012). Climatology and characteristics of stratospheric sudden warmings in the whole atmosphere community climate model. *Journal of Geophysical Research*, *117*, D04110. https://doi.org/10.1029/2011JD016840

Deser, C., Simpson, I. R., McKinnon, K. A., & Phillips, A. S. (2017). The Northern Hemisphere extratropical atmospheric circulation response to ENSO: How well do we know it and how do we evaluate models accordingly? *Journal of Climate*, *30*(13), 5059–5082. https://doi.org/10.1175/JCLI-D-16-0844.1

Domeisen, D. I. V., Garfinkel, C. I., & Butler, A. H. (2019). The teleconnection of El Nino southern oscillation to the stratosphere. *Reviews of Geophysics*, *57*, 5–47. https://doi.org/10.1029/2018RG000596

Fletcher, C. G., & Cassou, C. (2015). The dynamical influence of separate teleconnections from the Pacific and Indian Oceans on the Northern Annular Mode. *Journal of Climate*, *28*(20), 7985–8002. https://doi.org/10.1175/JCLI-D-14-00839.1

Fletcher, C. G., & Kushner, P. J. (2011). The role of linear interference in the annular mode response to tropical SST forcing. *Journal of Climate*, *24*(3), 778–794. https://doi.org/10.1175/2010JCLI3735.1

Fletcher, C. G., & Kushner, P. J. (2013). Linear interference and the Northern Annular Mode response to tropical SST forcing: Sensitivity to model configuration. *Journal of Geophysical Research: Atmospheres*, *118*, 4267–4279. https://doi.org/10.1002/jgrd.50385

Free, M., & Seidel, D. J. (2009). Observed El Niño-Southern Oscillation temperature signal in the stratosphere. *Journal of Geophysical Research*, *114*, D23108. https://doi.org/10.1029/2009JD012420

Frich, P., Alexander, L. V., Della-Marta, P., Gleason, B., Haylock, M., Tank, A. K., & Peterson, T. (2002). Observed coherent changes in climatic extremes during the second half of the twentieth century. *Climate Research*, *19*(3), 193–212. https://doi.org/10.3354/cr019193

Garcia, R. R., Marsh, D. R., Kinnison, D. E., Boville, B. A., & Sassi, F. (2007). Simulation of secular trends in the middle atmosphere, 1950-2003. *Journal of Geophysical Research*, *112*, D09301. https://doi.org/10.1029/2006JD007485

Garcia-Herrera, R., Calvo, N., Garcia, R. R., & Giorgetta, M. A. (2006). Propagation of ENSO temperature signals into the middle atmosphere: A comparison of two general circulation models and ERA-40 reanalysis data. *Journal of Geophysical Research*, *111*, D06101. https://doi.org/10.1029/2005JD006061

Garfinkel, C. I., Hurwitz, M. M., Oman, L. D., & Waugh, D. W. (2013). Contrasting effects of Central Pacific and Eastern Pacific El Niño on stratospheric water vapor. *Geophysical Research Letters*, *40*, 4115–4120. https://doi.org/10.1002/grl.50677

Garfinkel, C. I., Hurwitz, M. M., Waugh, D. W., & Butler, A. H. (2013). Are the teleconnections of Central Pacific and Eastern Pacific El Niño distinct in boreal wintertime? *Climate Dynamics*, *41*(7–8), 1835–1852. https://doi.org/10.1007/s00338-012-1570-2

Geng, X., Zhang, W., Stuecker, M. F., & Jin, F.-F. (2017). Strong sub-seasonal wintertime cooling over East Asia and Northern Europe associated with super El Niño events. *Science Reports Uk*, *7*(1), 3770. https://doi.org/10.1038/s41598-017-03977-2

Graf, H. F., & Zanchettin, D. (2012). Central Pacific El Nino, the "subtropical bridge," and Eurasian climate. *Journal of Geophysical Research*, *117*, D01102. https://doi.org/10.1029/2011JD016493

Graf, H. F., Zanchettin, D., Timmreck, C., & Bittner, M. (2014). Observational constraints on the tropospheric and near-surface winter signature of the Northern Hemisphere stratospheric polar vortex. *Climate Dynamics*, *43*(12), 3245–3266. https://doi.org/10.1007/s00382-014-2101-0

Hardiman, S. C., Dunstone, N. J., Scaife, A. A., Smith, D. M., Ineson, S., Lim, J., & Fereday, D. (2019). The impact of strong El Nino and La Nina events on the North Atlantic. *Geophysical Research Letters*, *46*, 2874–2883. https://doi.org/10.1029/2018GL081776

Hegyi, B. M., & Deng, Y. (2011). A dynamical fingerprint of tropical Pacific sea surface temperatures on the decadal-scale variability of cool-season Arctic precipitation. *Journal of Geophysical Research*, *116*, D20121. https://doi.org/10.1029/2011JD016001

Herceg-Bulić, I., Mezzina, B., Kucharski, F., Ruggieri, P., & King, M. P. (2017). Wintertime ENSO influence on late spring European climate: the stratospheric response and the role of North Atlantic SST. *International Journal of Climatology*, *37*, 87–108. https://doi.org/10.1002/joc.4980

Hoskins, B. J., James, I. N., & White, G. H. (1983). The shape, propagation and mean-flow interaction of large-scale weather systems. *Journal of the Atmospheric Sciences*, *40*(7), 1595–1612. https://doi.org/10.1175/1520-0469(1983)040<1595:TSPAMF>2.0.CO;2

Hurrell, J. W., Holland, M. M., Gent, P. R., Ghan, S., Kay, J. E., Kushner, P. J., et al. (2013). The Community Earth System Model: A framework for collaborative research. *Bulletin of the American Meteorological Society*, *94*(9), 1339–1360. https://doi.org/10.1175/Bams-D-12-00121.1

Ineson, S., & Scaife, A. A. (2009). The role of the stratosphere in the European climate response to El Niño. *Nature Geoscience*, *2*(1), 32–36. https://doi.org/10.1038/NGEO381

Jiménez-Esteve, B., & Domeisen, D. I. (2018). The tropospheric pathway of the ENSO–North Atlantic teleconnection. *Journal of Climate*, *31*(11), 4563–4584. https://doi.org/10.1175/JCLI-D-17-0716.1

Jin, F. F., & Hoskins, B. J. (1995). The direct response to tropical heating in a baroclinic atmosphere. *Journal of the Atmospheric Sciences*, *52*(3), 307–319. https://doi.org/10.1175/1520-0469(1995)052<0307:TDRTTH>2.0.CO;2

Kao, H. Y., & Yu, J. Y. (2009). Contrasting Eastern-Pacific and Central-Pacific types of ENSO. *Journal of Climate*, *22*(3), 615–632. https://doi.org/10.1175/2008JCLI2309.1

Kolstad, E. W., Breiteig, T., & Scaife, A. A. (2010). The association between stratospheric weak polar vortex events and cold air outbreaks in the Northern Hemisphere. *Quarterly Journal of the Royal Meteorological Society*, *136*(649), 886–893. https://doi.org/10.1002/qj.620

Kug, J. S., Jin, F. F., & An, S. I. (2009). Two types of El Nino events: Cold tongue El Nino and warm pool El Nino. *Journal of Climate*, *22*(6), 1499–1515. https://doi.org/10.1175/2008JCLI2624.1

Lan, X. Q., Chen, W., & Wang, L. (2012). Quasi-stationary planetary wave-mean flow interactions in the Northern Hemisphere stratosphere and their responses to ENSO events. *Science China Earth Sciences*, *55*(3), 405–417. https://doi.org/10.1007/S11430-011-4345-4

Larkin, N. K., & Harrison, D. E. (2005). On the definition of El Niño and associated seasonal average US weather anomalies. *Geophysical Research Letters*, *32*, L13705. https://doi.org/10.1029/2005GL022738

Lee, S. H., & Butler, A. H. (2020). The 2018–2019 Arctic stratospheric polar vortex. *Weather*, *75*(2), 52–57. https://doi.org/10.1002/wea.3643

L'Heureux, M. L., Takahashi, K., Watkins, A. B., Barnston, A. G., Becker, E. J., Di Liberto, T. E., et al. (2017). Observing and predicting the 2015/16 El Niño. *Bulletin of the American Meteorological Society*, *98*(7), 1363–1382. https://doi.org/10.1175/BAMS-D-16-0009.1

Li, Y., & Lau, N.-C. (2012). Impact of ENSO on the atmospheric variability over the North Atlantic in late winter—Role of transient eddies. *Journal of Climate*, *25*(1), 320–342. https://doi.org/10.1175/JCLI-D-11-00037.1

Lorenz, D. J., & Hartmann, D. L. (2001). Eddy–Zonal Flow Feedback in the Southern Hemisphere. *Journal of the Atmospheric Sciences*, *58*(21), 3312–3327. https://doi.org/10.1175/1520-0469(2001)058%3C3312:ezffit%3E2.0.co;2

Manzini, E., Giorgetta, M. A., Esch, M., Kornblueh, L., & Roeckner, E. (2006). The influence of sea surface temperatures on the northern winter stratosphere: Ensemble simulations with the MAECHAM5 model. *Journal of Climate*, *19*(16), 3863–3881. https://doi.org/10.1175/Jcli3826.1

Marsh, D. R., Mills, M. J., Kinnison, D. E., Lamarque, J. F., Calvo, N., & Polvani, L. M. (2013). Climate change from 1850 to 2005 simulated in CESM1(WACCM). *Journal of Climate*, *26*(19), 7372–7391. https://doi.org/10.1175/JCLI-D-12-00558.1

Merkel, U., & Latif, M. (2002). A high resolution AGCM study of the El Niño impact on the North Atlantic/European sector. *Geophysical Research Letters*, *29*(9), 1291. https://doi.org/10.1029/2001GL013726

Murakami, M. (1979). Large-scale aspects of deep convective activity over the GATE area. *Monthly Weather Review*, *107*(8), 994–1013. https://doi.org/10.1175/1520-0493(1979)107<0994:LSAODC>2.0.CO;2

Newman, M., & Sardeshmukh, P. D. (2008). Tropical and stratospheric influences on extratropical short-term climate variability. *Journal of Climate*, *21*(17), 4326–4347. https://doi.org/10.1175/2008JCLI2118.1

Ortiz Bevia, M. J., Perez-Gonzalez, I., Alvarez-Garcia, F. J., & Gershunov, A. (2010). Nonlinear estimation of El Niño impact on the North Atlantic winter. *Journal of Geophysical Research*, *115*, D21123. https://doi.org/10.1029/2009JD013387

Perlwitz, J., & Graf, H.-F. (1995). The statistical connection between tropospheric and stratospheric circulation of the Northern Hemisphere in winter. *Journal of Climate*, *8*(10), 2281–2295. https://doi.org/10.1175/1520-0442(1995)008<2281:TSCBTA>2.0.CO;2

Plumb, R. A. (1985). On the three-dimensional propagation of stationary waves. *Journal of the Atmospheric Sciences*, *42*(3), 217–229. https://doi.org/10.1175/1520-0469(1985)042<0217:OTTDPO>2.0.CO;2

Pohlmann, H., & Latif, M. (2005). Atlantic versus Indo-Pacific influence on Atlantic-European climate. *Geophysical Research Letters*, *32*, L05707. https://doi.org/10.1029/2004GL021316

Rao, J., & Ren, R. C. (2016a). Asymmetry and nonlinearity of the influence of ENSO on the northern winter stratosphere: 1. Observations. *Journal of Geophysical Research – Atmospheres*, *121*, 9000–9016. https://doi.org/10.1002/2015JD024520

Rao, J., & Ren, R. C. (2016b). Asymmetry and nonlinearity of the influence of ENSO on the northern winter stratosphere: 2. Model study with WACCM. *Journal of Geophysical Research-Atmospheres*, *121*, 9017–9032. https://doi.org/10.1002/2015JD024521

Rayner, N. A., Parker, D. E., Horton, E. B., Folland, C. K., Alexander, L. V., Rowell, D. P., et al. (2003). Global analyses of sea surface temperature, sea ice, and night marine air temperature since the late nineteenth century. *Journal of Geophysical Research*, *108*(D14), 4407. https://doi.org/10.1029/2002JD002670

Ren, H. L., & Jin, F. F. (2013). Recharge oscillator mechanisms in two types of ENSO. *Journal of Climate*, *26*(17), 6506–6523. https://doi.org/10.1175/JCLI-D-12-00601.1

Ren, R. C., Cai, M., Xiang, C. Y., & Wu, G. X. (2012). Observational evidence of the delayed response of stratospheric polar vortex variability to ENSO SST anomalies. *Climate Dynamics*, *38*(7–8), 1345–1358. https://doi.org/10.1007/s00382-011-1137-7

Richter, J. H., Deser, C., & Sun, L. (2015). Effects of stratospheric variability on El Niño teleconnections. *Environmental Research Letters*, *10*(12), 124021.

Shaman, J., & Tziperman, E. (2005). The effect of ENSO on Tibetan Plateau snow depth: A stationary wave teleconnection mechanism and implications for the South Asian monsoons. *Journal of Climate*, *18*(12), 2067–2079. https://doi.org/10.1175/JCLI3391.1

Simmons, A., Uppala, S., & Dee, D. (2007). Update on ERA-Interim. *ECMWF Newsletter*, *111*(5).

Simmons, A., Uppala, S., Dee, D., & Kobayashi, S. (2007). ERA-Interim: New ECMWF reanalysis products from 1989 onwards. *ECMWF newsletter*, *110*(110), 25–35.

Simpson, I. R., Hitchcock, P., Shepherd, T. G., & Scinocca, J. F. (2011). Stratospheric variability and tropospheric annular-mode timescales. *Geophysical Research Letters*, *38*, L20806. https://doi.org/10.1029/2011GL049304

Smith, K. L., Fletcher, C. G., & Kushner, P. J. (2010). The role of linear interference in the annular mode response to extratropical surface forcing. *Journal of Climate*, *23*(22), 6036–6050. https://doi.org/10.1175/2010JCLI3606.1

Song, Y., & Robinson, W. A. (2004). Dynamical mechanisms for stratospheric influences on the troposphere. *Journal of the Atmospheric Sciences*, *61*(14), 1711–1725. https://doi.org/10.1175/1520-0469(2004)061<1711:DMFSIO>2.0.CO;2

Takaya, K., & Nakamura, H. (2001). A formulation of a phase-independent wave-activity flux for stationary and migratory quasigeostrophic eddies on a zonally varying basic flow. *Journal of the Atmospheric Sciences*, *58*(6), 608–627. https://doi.org/10.1175/1520-0469(2001)058<0608:AFOAPI>2.0.CO;2

Thompson, D. W., Baldwin, M. P., & Wallace, J. M. (2002). Stratospheric connection to Northern Hemisphere wintertime weather: Implications for prediction. *Journal of Climate*, *15*(12), 1421–1428. https://doi.org/10.1175/1520-0442(2002)015<1421:SCTNHW>2.0.CO;2

Tomassini, L., Gerber, E. P., Baldwin, M. P., Bunzel, F., & Giorgetta, M. (2012). The role of stratosphere-troposphere coupling in the occurrence of extreme winter cold spells over northern Europe. *Journal of Advances in Modeling Earth Systems*, *4*, M00A03. https://doi.org/10.1029/2012MS000177

Toniazzo, T., & Scaife, A. A. (2006). The influence of ENSO on winter North Atlantic climate. *Geophysical Research Letters*, *33*, L24704. https://doi.org/10.1029/2006gl027881

Trascasa-Castro, P., Maycock, A. C., Yiu, Y. Y. S., & Fletcher, J. K. (2019). On the linearity of the stratospheric and euro-Atlantic sector response to ENSO. *Journal of Climate*, *32*(19), 6607–6626. https://doi.org/10.1175/JCKI-D-18-0746.1

Trenberth, K. E. (1986). An assessment of the impact of transient eddies on the zonal flow during a blocking episode using localized Eliassen-palm flux diagnostics. *Journal of the Atmospheric Sciences*, *43*(19), 2070–2087. https://doi.org/10.1175/1520-0469(1986)043<2070:AAOTIO>2.0.CO;2

Uppala, S., Dee, D., Kobayashi, S., Berrisford, P., & Simmons, A. (2008). Towards a climate data assimilation system: Status update of ERA-interim. *ECMWF newsletter*, *115*(7), 12–18.
Vallis, G. K. (2013). *Atmospheric and Oceanic Fluid Dynamics*. (p. 769). Cambridge: Cambridge University Press.
Wu, Y., & Smith, K. L. (2016). Response of Northern Hemisphere midlatitude circulation to Arctic amplification in a simple atmospheric general circulation model. *Journal of Climate*, *29*(6), 2041–2058. https://doi.org/10.1175/JCLI-D-15-0602.1
Xie, F., Li, J., Tian, W., Feng, J., & Huo, Y. (2012). Signals of El Niño Modoki in the tropical tropopause layer and stratosphere. *Atmospheric Chemistry and Physics*, *12*(11), 5259–5273. https://doi.org/10.5194/acp-12-5259-2012
Yu, J. Y., & Kao, H. Y. (2007). Decadal changes of ENSO persistence barrier in SST and ocean heat content indices: 1958–2001. *Journal of Geophysical Research*, *112*, D13106. https://doi.org/10.1029/2006JD007654
Zhang, J., Tian, W., Chipperfield, M. P., Xie, F., & Huang, J. (2016). Persistent shift of the Arctic polar vortex towards the Eurasian continent in recent decades. *Nature Climate Change*, *6*(12), 1094–1099.
Zhang, J., Tian, W., Wang, Z., Xie, F., & Wang, F. (2015). The influence of ENSO on northern midlatitude ozone during the winter to spring transition. *Journal of Climate*, *28*(12), 4774–4793. https://doi.org/10.1175/JCLI-D-14-00615.1
Zhang, K., Wang, T., Xu, M., & Zhang, J. (2019). Influence of wintertime polar vortex variation on the climate over the North Pacific during late winter and spring. *Atmosphere*, *10*(11), 670. https://doi.org/10.3390/atmos10110670
Zhang, X., Hegerl, G., Zwiers, F. W., & Kenyon, J. (2005). Avoiding inhomogeneity in percentile-based indices of temperature extremes. *Journal of Climate*, *18*(11), 1641–1651. https://doi.org/10.1175/JCLI3366.1
Zhou, X., Li, J. P., Xie, F., Chen, Q. L., Ding, R. Q., Zhang, W. X., & Li, Y. (2018). Does extreme El Nino have a different effect on the stratosphere in boreal winter than its moderate counterpart? *Journal of Geophysical Research-Atmospheres*, *31*, 929–943. https://doi.org/10.1002/2017JD028064